MEMBRANES

Sieving hydrogen isotopes through two-dimensional crystals

M. Lozada-Hidalgo,[1]*† S. Hu,[1]† O. Marshall,[1] A. Mishchenko,[1] A. N. Grigorenko,[1] R. A. W. Dryfe,[2] B. Radha,[1] I. V. Grigorieva,[1] A. K. Geim[1]*

One-atom-thick crystals are impermeable to atoms and molecules, but hydrogen ions (thermal protons) penetrate through them. We show that monolayers of graphene and boron nitride can be used to separate hydrogen ion isotopes. Using electrical measurements and mass spectrometry, we found that deuterons permeate through these crystals much slower than protons, resulting in a separation factor of ≈10 at room temperature. The isotope effect is attributed to a difference of ≈60 milli−electron volts between zero-point energies of incident protons and deuterons, which translates into the equivalent difference in the activation barriers posed by two-dimensional crystals. In addition to providing insight into the proton transport mechanism, the demonstrated approach offers a competitive and scalable way for hydrogen isotope enrichment.

Unlike conventional membranes used for sieving atomic and molecular species, monolayers of graphene and hexagonal boron nitride (hBN) exhibit subatomic selectivity (1–5). They are permeable to thermal protons (5)—and electrons (6)—but in the absence of structural defects, are completely impermeable to larger, atomic species (1–5, 7–10). Proton transport through these two-dimensional (2D) crystals is a thermally activated process, with energy barriers E of ≈0.3 and 0.8 eV for monolayers of hBN and graphene, respectively, that were attributed to different densities of their electron clouds that must be pierced by incident protons (5). Investigating whether deuterons—nuclei of the heavier hydrogen isotope, deuterium (D)—can pass through atomically thin crystals is of interest for elucidating the proton transport mechanism (11–14). If the 2D membranes can distinguish between the two nuclei (hydrons), this would also be of interest for applications, as hydrogen isotopes are important for various analytical and tracing technologies, and heavy water is used in huge quantities by nuclear fission plants. The existing H/D separation techniques, such as water–hydrogen sulfide exchange and cryogenic distillation (15, 16), are extremely energy intensive and show low separation factors (<2.5), which stimulates continuous search for alternative technologies (15–21) [see supplementary materials (22)].

We investigated whether deuterons (D$^+$) permeate through 2D crystals differently from protons (H$^+$) studied previously (5). Two complementary approaches, electrical conductivity measurements and gas flow detection by mass spectrometry (22), were explored. In the first approach, graphene and hBN monocrystals were mechanically exfoliated and suspended over micrometer-sized holes etched in silicon wafers (fig. S1). To measure 2D crystals' hydron conductivity σ, both sides of the resulting membranes were coated with a proton-conducting polymer—Nafion (23)—and electrically contacted with Pd electrodes that converted electron into hydron flow (Fig. 1A, inset). The measurements were performed in an atmosphere of either H$_2$-Ar/H$_2$O or D$_2$-Ar/D$_2$O in 100% humidity at room temperature. The different atmospheres turned Nafion into a proton (H-Nafion) or deuteron (D-Nafion) (24) conductor with little presence of the other isotope (fig. S2). For reference, similar devices but without 2D membranes were fabricated. The latter exhibited similar conductance, whether H- or D-Nafion was used, and it was typically 100 times higher than that found for devices incorporating 2D crystals. This shows that the series contribution to our device resistances from Nafion and Pd contacts could be neglected (5, 22).

For both H- and D-Nafion devices, the measured current I varied linearly with applied bias voltage V (Fig. 1A), but different 2D crystals showed widely different areal conductivities, σ = I/SV, where S is the membrane area (Fig. 1B). Monolayer hBN exhibited the highest proton conductivity, σ_H, followed by bilayer hBN and monolayer graphene (Fig. 1B), in agreement with the previous work (5). σ was markedly smaller (by a factor of 10) for D-Nafion devices compared to their H-Nafion counterparts, independent of the tested 2D crystal (Fig. 1B). Furthermore, we carried out similar measurements for Pt-activated membranes (hBN and graphene monolayers covered with a discontinuous layer of Pt to enhance hydron transport) (22) and, again, the conductivity for deuterons, σ_D, was always about $\frac{1}{10}$ of that for protons (fig. S3). This pronounced isotope effect is unexpected, and its independence of 2D barrier height is particularly puzzling. These observations do not follow from either previous experiments (5, 10) or existing theories (7–9) in which the calculated

barriers arise from the interaction of a positive point charge with the 2D crystals' electron clouds, and the hydron mass is assumed to be irrelevant.

In our second series of experiments, graphene membranes were used to separate a liquid cell and a vacuum chamber (Fig. 2A). On the liquid side (input), graphene was coated with a thin Nafion layer that faced a reservoir containing a proton-deuteron electrolyte (HCl in H$_2$O mixed with DCl in D$_2$O). The atomic fractions of H$^+$ and D$^+$ in this mixture could be changed as required. The other side of graphene, decorated with Pt nanoparticles, faced the vacuum chamber equipped with a mass spectrometer (5, 22). A bias—typically, ≲2 V to avoid damage to our devices (fig. S6)—was applied directly between graphene and the electrolyte (Fig. 2A and fig. S1). This setup effectively represents an electrochemical pump (25, 26) in which the graphene membrane serves simultaneously as a semitransparent hydron barrier and a drain electrode for protons and deuterons. The gas and liquid impermeability was checked for each experimental device with a He leak detector. The key advantage of mass spectrometry with respect to our electrical measurements is that it can distinguish between different hydron species. This allowed us to determine directly the composition of output gas flows for different input electrolytes. Unfortunately, mass spectrometry is also much less sensitive than electrical measurements and, therefore, large hydron fluxes were necessary to probe the current-induced gas flows in the presence of a fluctuating background in the spectrometer (22). To compensate for the lower sensitivity, we used high I and graphene crystals as large as possible, fabricating membranes up to 50 μm in diameter. This allowed flows >>10^{10} molecules/s for all three possible gases—H$_2$, D$_2$, and protium deuteride (HD)—which appeared on the vacuum side (Fig. 2B and fig. S4).

We found that the flow of each of the gases varied linearly with I, as expected, but depended strongly on the relative concentrations ([H$^+$]:[D$^+$]) of hydrons in the input electrolyte ([H$^+$] + [D$^+$] = 100%). This is illustrated in Fig. 2B for the case of D$_2$ and further in figs. S4 to S6. By measuring such flow-current dependences for different [H$^+$]:[D$^+$] inputs, we determined the percentage of H$_2$, D$_2$, and HD in output flows (Fig. 2C). These data are easily converted into the percentage of H and D atoms at the output of our electrochemical pump as a function of [H$^+$] or [D$^+$] at its input. We find that the output fraction of atomic hydrogen is disproportionally high with respect to the input fraction of protons (Fig. 2D). For example, for equal amounts of protons and deuterons at the input, H accounted for ≈95% of the atoms in the output flow—that is, graphene membranes efficiently sieved out deuterium. As a control experiment, we repeated the same measurements substituting graphene with porous carbon and found no preferential flow of protons or deuterons, as expected (fig. S5). To quantify the observed sieving efficiencies, we calculated the separation factor α. The data in Fig. 2D yield α ≈ 10, in good

[1]School of Physics and Astronomy, University of Manchester, Manchester M13 9PL, UK. [2]School of Chemistry, University of Manchester, Manchester M13 9PL, UK.
*Corresponding author. E-mail: marcelo.lozadahidalgo@manchester.ac.uk (M.L.-H.); geim@manchester.ac.uk (A.K.G.)
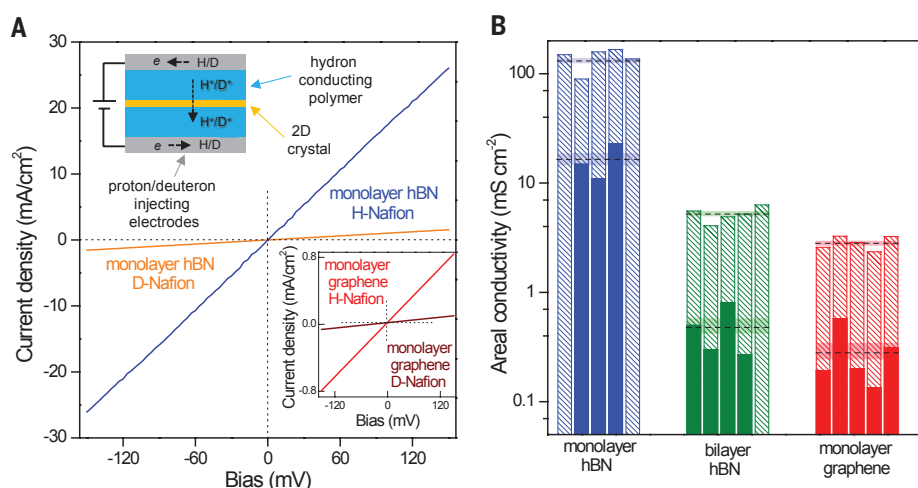†These authors contributed equally to this work.

Fig. 1. Proton versus deuteron conductivities of 2D crystals. (**A**) Examples of *I-V* characteristics for hydron transport through monolayers of hBN (main panel) and graphene (lower inset). Top inset: Schematics of the experimental setup. Pd electrodes supply protons or deuterons into H- or D-Nafion; 2D crystals serve as barriers for hydrons. (**B**) Proton and deuteron conductivities (shaded and solid bars, respectively) for the most hydron-conductive 2D crystals. Each bar (solid or shaded) corresponds to a different device (nearly 30 are shown). The dashed lines mark the average conductivities for the six sets of devices, and the shaded areas around them show the standard errors.
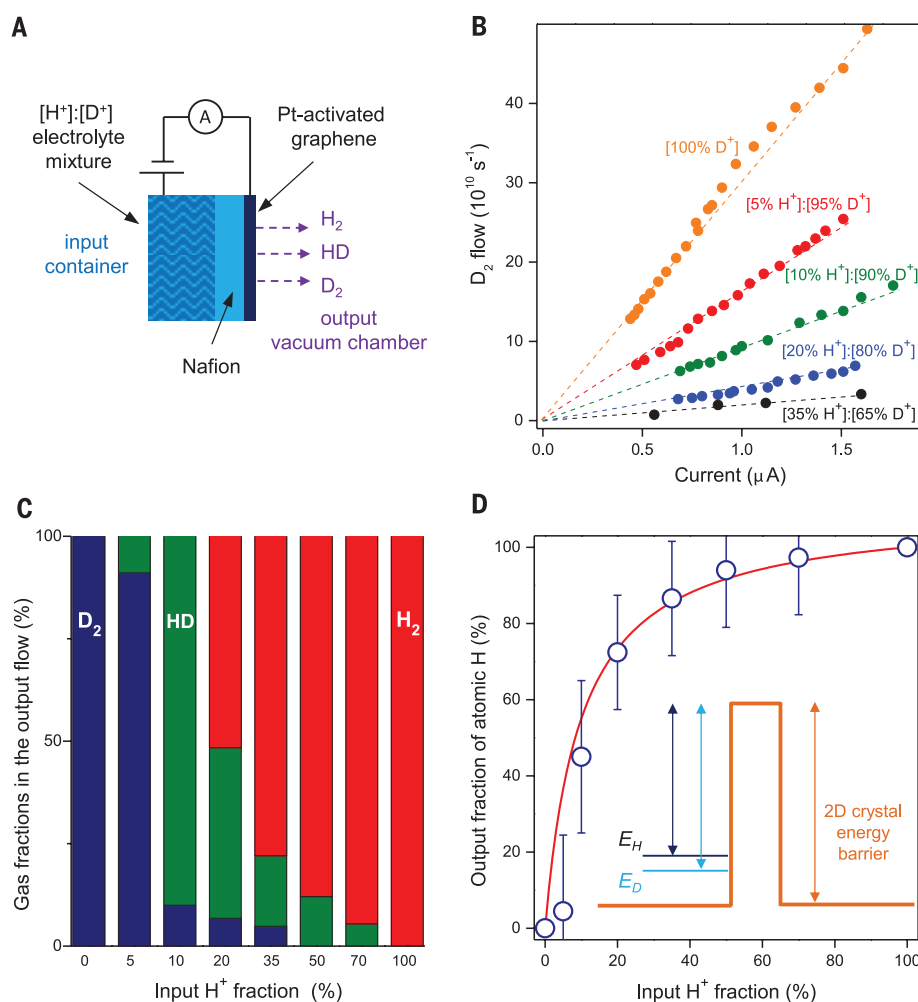

Fig. 2. Isotope separation by electrochemical pumping of hydrons through graphene. (**A**) Schematic of our mass spectrometry setup. (**B**) D₂ flow versus applied current for various proton-deuteron fractions in the input electrolyte. The dashed lines are linear fits. (**C**) Relative fractions of H₂, HD, and D₂ in the output flow for eight different compositions of the input electrolyte. (**D**) Fraction of H atoms at the output for different [H⁺] inputs. Inset: Schematic of the energy barrier presented by a 2D crystal for proton and deuteron transfer. The black and blue horizontal lines indicate zero-point states of protons and deuterons, respectively, in Nafion and water. The solid red curve shows the separation dependence expected for the known difference $E_D - E_H = 60$ meV, with no fitting parameters.

agreement with the value found from the ratio σ_H/σ_D in our conductivity measurements (*22*).

To explain the observed isotope effect, we first recall that proton permeation through 2D crystals is a thermally activated process (*5, 9*). Therefore, if we neglect—to a first approximation (*22*)—the pre-exponential factor in the Arrhenius equation, our results can equivalently be described in terms of the energy barriers E_H and E_D presented by 2D crystals to proton and deuteron transport, respectively. Accordingly, we can write $\sigma_H/\sigma_D \approx \exp(\Delta E/k_B T)$, where $\Delta E = E_D - E_H$ and k_B is Boltzmann's constant. Although E_H and E_D obviously determine the hydron permeability of 2D crystals (*5, 7–9*), their selectivity depends only on ΔE. Statistical analysis of the data in Fig. 1B yields $\sigma_H/\sigma_D \approx 10 \pm 0.8$, which translates into $\Delta E \approx 60 \pm 2$ meV for all the tested 2D membranes. Furthermore, the same value of ΔE allows us to describe quantitatively the selectivity found by the mass spectrometry measurements. As shown in supplementary materials, the protium output is given by [H] = [H⁺]/{[H⁺]+exp($-\Delta E/k_B T$)[D⁺]}. This dependence is plotted in Fig. 2D using $\Delta E = 60$ meV and shows excellent agreement with the experiment.

Where does the difference between E_H and E_D come from, and why is it the same for all the tested 2D membranes despite their hydron conductivities being different by many orders of magnitude? The protons and deuterons in our experiments move not in vacuum but along hydrogen-bonded networks provided by sulfonate groups (SO₃⁻) and water in Nafion (*23*). It is reasonable to expect that, before jumping through 2D crystals, hydrons remain transiently bonded to sulfonate and water groups and, accordingly, this presents the initial state in the transfer process (Fig. 2D, inset). The zero-point energies of these hydrogen-oxygen bonds are ≈0.2 eV for protons and ≈0.14 eV for deuterons (*11, 22*). As illustrated in Fig. 2D, zero-point oscillations effectively reduce the activation barrier with respect to vacuum by 0.2 eV for protons, whereas for deuterons the reduction is smaller by 60 meV. This explanation is

consistent with all the experimental evidence. We expect the same-strength isotope effect if the 2D crystals are combined with other proton conductors based on oxides (13, 25–28), and the separation factor should be even larger for proton-conducting media with stronger hydrogen bonds; for example, in fluorides (28).

The above explanation allows for several observations about proton transport through 2D crystals. First, it partially explains the disagreement between the experiment (5) and theory (5, 8–10) in the absolute value of E_H for graphene: Zero-point oscillations reduce the activation barrier by ≈0.2 eV compared to theoretical values. We speculate that the remaining differences [<20% in the case of (8)] may be accounted for by considering other effects of the surrounding media (for example, two-body processes involving a distortion of the electron clouds by protons residing at the Nafion-graphene interface). Second, the experiments confirm that hydrogen chemisorption to 2D crystals is not the limiting step in the transfer process because, otherwise, the isotope effect would be different for hBN and graphene. Third, the described sieving mechanism implies α ≈30 for tritium-hydrogen separation. Fourth, it is quite remarkable that zero-point oscillations, a purely quantum effect, can still dominate room-temperature transport properties of particles 4000 times heavier than electrons.

The observed large α compares favorably with sieving efficiencies of the existing methods for hydrogen isotope separation (15–20). The high proton conductivity exhibited by graphene and boron nitride monolayers, comparable to that of commercial Nafion films (5, 22), makes them potentially interesting for such applications. In this respect, the increasing availability of graphene grown by chemical vapor deposition (CVD) (29, 30) provides a realistic prospect of scaling up the described devices from micrometer sizes to those required for industrial uses. Indeed, although micromechanical cleavage allows 2D membranes of highest quality, the approach is not scalable. As a proof of concept, we repeated the mass spectrometry measurements using centimeter-sized membranes made from CVD graphene and achieved the same α ≈ 10 (fig. S7). Notably, this shows that macroscopic cracks and pinholes present in CVD graphene do not affect the efficiency, because hydrons are electrochemically pumped only through the graphene areas that are electrically contacted (22). Furthermore, we estimate the energy costs associated with this isotope separation method as ≈0.3 kWh per kilogram of feed water (22), appreciably lower than costs of the existing enrichment processes (15, 16). All this comes on top of the fundamentally simple and robust sieving mechanism, potentially straightforward setups, and the need for only water at the input without the use of chemical compounds (16).

REFERENCES AND NOTES

1. J. S. Bunch et al., Nano Lett. **8**, 2458–2462 (2008).
2. S. P. Koenig, L. Wang, J. Pellegrino, J. S. Bunch, Nat. Nanotechnol. **7**, 728–732 (2012).
3. O. Leenaerts, B. Partoens, F. M. Peeters, Appl. Phys. Lett. **93**, 193107 (2008).
4. V. Berry, Carbon **62**, 1–10 (2013).
5. S. Hu et al., Nature **516**, 227–230 (2014).
6. L. Britnell et al., Nano Lett. **12**, 1707–1710 (2012).
7. L. Tsetseris, S. T. Pantelides, Carbon **67**, 58–63 (2014).
8. W. L. Wang, E. Kaxiras, New J. Phys. **12**, 125012 (2010).
9. M. Miao, M. B. Nardelli, Q. Wang, Y. Liu, Phys. Chem. Chem. Phys. **15**, 16132–16137 (2013).
10. J. L. Achtyl et al., Nat. Commun. **6**, 6539 (2015).
11. K. B. Wiberg, Chem. Rev. **55**, 713–743 (1955).
12. B. E. Conway, Proc. R. Soc. A Math. Phys. Eng. Sci. **256,** 128–144 (1960).
13. K. D. Kreuer, A. Fuchs, J. Maier, Solid State Ion. **77**, 157–162 (1995).
14. A. Paris et al., Adv. Funct. Mater. **23**, 1628–1635 (2013).
15. H. K. Rae, Ed., Separation of Hydrogen Isotopes (ACS Symposium Series, Washington, DC, 1978).
16. A. I. Miller, Can. Nucl. Soc. Bull. **22**, 1–14 (2001).
17. J. J. M. Beenakker, V. D. Borman, S. Y. Krylov, Chem. Phys. Lett. **232**, 379–382 (1995).
18. X. Zhao, S. Villar-Rodil, A. J. Fletcher, K. M. Thomas, J. Phys. Chem. B **110**, 9947–9955 (2006).
19. B. E. Conway, Proc. R. Soc. London Ser. A **247**, 400–419 (1958).
20. J. H. Rolston, J. Den Hartog, J. P. Butler, J. Phys. Chem. **80**, 1064–1067 (1976).
21. J. B. Marling, I. P. Herman, S. J. Thomas, J. Chem. Phys. **72**, 5603–5634 (1980).
22. See supplementary materials on Science Online.
23. K. A. Mauritz, R. B. Moore, Chem. Rev. **104**, 4535–4586 (2004).
24. K. W. Feindel, S. H. Bergens, R. E. Wasylishen, J. Power Sources **173**, 86–95 (2007).
25. T. Hibino, K. Mizutani, H. Iwahara, J. Electrochem. Soc. **140**, 2588 (1993).
26. K. D. Kreuer, Chem. Mater. **8**, 610–641 (1996).
27. D. Marx, M. E. Tuckerman, J. Hutter, M. Parrinello, Nature **397**, 601–604 (1999).
28. D. Marx, ChemPhysChem **7**, 1848–1870 (2006).
29. A. Reina et al., Nano Lett. **9**, 30–35 (2009).
30. K. S. Kim et al., Nature **457**, 706–710 (2009).

ORGANIC CHEMISTRY

Catalytic conjunctive cross-coupling enabled by metal-induced metallate rearrangement

Liang Zhang, Gabriel J. Lovinger, Emma K. Edelstein, Adam A. Szymaniak, Matteo P. Chierchia, James P. Morken*

Transition metal catalysis plays a central role in contemporary organic synthesis. Considering the tremendously broad array of transition metal–catalyzed transformations, it is remarkable that the underlying elementary reaction steps are relatively few in number. Here, we describe an alternative to the organometallic transmetallation step that is common in many metal-catalyzed reactions, such as Suzuki-Miyaura coupling. Specifically, we demonstrate that vinyl boronic ester ate complexes, prepared by combining organoboronates and organolithium reagents, engage in palladium-induced metallate rearrangement wherein 1,2-migration of an alkyl or aryl group from boron to the vinyl α-carbon occurs concomitantly with C–Pd σ-bond formation. This elementary reaction enables a powerful cross-coupling reaction in which a chiral Pd catalyst merges three simple starting materials—an organolithium, an organoboronic ester, and an organotriflate—into chiral organoboronic esters with high enantioselectivity.

Organoboronic acids and their derivatives are widely available and broadly useful starting materials for organic synthesis (1). In addition to being environmentally benign and generally inexpensive, these reagents exhibit a near-ideal balance of stability and reactivity. Although chemically and configurationally stable, organoboronic esters engage in a broad array of carbon-carbon and carbon-heteroatom bond-forming processes upon activation. The most commonly practiced such reaction is the transition metal–catalyzed Suzuki-Miyaura cross-coupling reaction between organic electrophiles and organoboron compounds (2). In broad strokes, the mechanism of the Suzuki-Miyaura reaction involves a sequence of (i) oxidative addition between a metal catalyst and the electrophile, (ii) transmetallation with the organoboron reagent, and (iii) reductive elimination of the C-C bonded product (3). Here, we used an alternative pathway to the organoboron transmetallation step. The overall putative catalytic cycle enables a class of organoboron cross-coupling that we term "conjunctive cross-coupling" (Fig. 1A) because it merges

Department of Chemistry, Boston College, Chestnut Hill, MA 02467, USA.
*Corresponding author. E-mail: morken@bc.edu